

On Performance of Vector OFDM with Zero-Forcing Receiver

Yabo Li , Ibo Ngehani,
Dept. of Info. Sci. and Elec. Eng.,
Zhejiang University,
Hangzhou, Zhejiang, P.R.China.
e-mail: yaboli@zju.edu.cn

Xiang-Gen Xia
Dept. of Elec. and Comp. Eng.,
University of Delaware, Newark, DE 19716 U.S.A.
Chonbuk National University, Jeonju, South Korea.
e-mail: xxia@ee.udel.edu

Abstract—Vector OFDM (Orthogonal Frequency Division Multiplexing) for single transmit antenna systems is a general transmission scheme, where OFDM and SC-FDE (Single-Carrier Frequency Domain Equalization) can be treated as two special/extreme cases. Due to its flexibility, it has drawn more and more attention recently. So far, all the studies about Vector OFDM assume the ML (Maximum Likelihood) receiver. In this paper, we investigate the performance of Vector OFDM with the ZF (Zero-Forcing) receiver. We firstly show that for the ZF receiver, all the transmitted symbols have equal performance. This is different from the Vector OFDM with ML receiver, where different VBs may have different coding gain, and thus may have different performances. We then analyze the diversity order for Vector OFDM with ZF receiver, and show that the diversity order equals 1 and the performance is the same as the conventional OFDM at high SNR.

Index Terms—Diversity order, linear receiver, multipath diversity, OFDM, SC-FDE, signal space diversity, Vector OFDM, ZF.

I. INTRODUCTION

OFDM (Orthogonal Frequency Division Multiplexing) [1] [2], as a low complexity transmission scheme in multipath channels, has been widely adopted in the next generation wireless communication systems such as WiMAX [3], LTE [4], and WiFi [5]. Although OFDM has low complexity, without coding, it cannot exploit the multipath diversity, and therefore performs worse than single carrier transmission with time domain equalizers. Furthermore, OFDM has very high PAPR (Peak-to-Average Power Ratio), which puts high requirements on the PA (Power Amplifier) and increases the transceiver cost [6]. To mitigate PAPR while retaining low complexity, SC-FDE (Single-Carrier Frequency Domain Equalization) [7]–[10] was proposed. At the transmitter, SC-FDE removes the IFFT (Inverse Fast Fourier Transform) block of OFDM, so the PAPR is reduced. At the receiver, SC-FDE first does FFT and channel equalization in the frequency domain, and then does IFFT and demodulation/detection in the time domain. Compared with OFDM, it can be seen that SC-FDE has unbalanced transmitter and receiver complexities. It is further shown that for high order signal constellations, such as 64QAM, SC-FDE suffers performance loss [11]. Therefore, it is commonly agreed that OFDM is more suitable for high data rate and high cost transceivers, while SC-FDE is more suitable

for low data rate and low cost transceivers. For example, in LTE [4], OFDM/OFDMA (Orthogonal Frequency Division Multiple Access) is used in the downlink, where high data rate is more important, and SC-FDE/SC-FDMA (Single-Carrier Frequency Division Multiple Access) is used in the uplink, where low cost is more important. In the next generation millimeter-wave based WiFi, i.e. IEEE 802.11ad [5], both OFDM based PHY (Physical Layer) and SC-FDE based PHY are defined, where the OFDM based PHY is for high data rate devices, and the used constellation can be up to 64QAM, while the SC-FDE based PHY is for low data rate, low cost and low power devices. The definition of two PHY schemes complicates the system design.

Vector OFDM (V-OFDM), first proposed by Xia [12] to reduce the cyclic prefix (CP) overhead and the IFFT size of a single transmit antenna OFDM system, can be treated as a general transmission scheme, where OFDM and SC-FDE are just two special/extreme cases. So, V-OFDM bridges the gap between OFDM and SC-FDE. By adjusting parameters, the V-OFDM based system can be adapted to cater to different system design requirements, such as PAPR, transceiver cost, data rate, performance, etc. Thus, compared with the two PHY schemes in IEEE 802.11ad [5], V-OFDM is an attractive alternative. With regards to different system design aspects of V-OFDM, [13] analyzed the synchronization and guard band settings, [15] introduced the vector channel allocation, [14] exploited the turbo principle to do iterative demodulation and decoding, [16] observed that different vector blocks (VB) may have different performances when the ML (Maximum Likelihood) receiver is used and further proposed a constellation rotation scheme to ensure consistent performance for different VBs, [17] thoroughly investigated the V-OFDM performance under multipath Rayleigh fading with the ML receiver.

So far, all the discussions about V-OFDM, such as [12]–[17], are based on the ML receiver, whose complexity increases exponentially with the size of the VB defined in V-OFDM, though the performance increases with the size of the VB as well. It is still unknown how V-OFDM performs with the ZF (Zero Forcing) receivers. In this paper, we investigate the performance of V-OFDM with the ZF receiver. In the following, we call the V-OFDM with ML and ZF receivers ML-V-OFDM and ZF-V-OFDM, respectively.

The remainder of the paper is organized as follows. In Section II, the system model of V-OFDM is introduced. In Section III, different detection algorithms are introduced and the characteristics of the detection SNRs are analyzed. In Section IV, the equal performance of different VBs for ZF-V-OFDM is shown. In Section V, the diversity orders of ZF-V-OFDM is analyzed. In Section VI, some numerical results are provided to validate the theoretical analysis.

II. VECTOR OFDM SYSTEM MODEL

Similar to conventional OFDM, in V-OFDM, the modulated symbols are processed block-by-block. Assume that there are $N = LM$ modulated symbols in one block, and denote them as $\{x_n\}_{n=0}^{N-1}$. Different from conventional OFDM, V-OFDM further divides the length N block into L VBs, where each VB has size M . Denote the l -th VB as

$$\mathbf{x}_l = [x_{lM}, x_{lM+1}, \dots, x_{lM+M-1}]^T, \quad l = 0, 1, \dots, L-1.$$

We call \mathbf{x}_l the l -th transmit VB. Instead of doing IFFT of size N as in conventional OFDM, V-OFDM does component-wise vector IFFT of size L over the VBs, i.e., calculates

$$\bar{\mathbf{x}}_q = \frac{1}{L} \sum_{l=0}^{L-1} \mathbf{x}_l e^{j\frac{2\pi ql}{L}}, \quad q = 0, 1, \dots, L-1.$$

$\bar{\mathbf{x}}_q$ is a column vector of size M and is denoted as

$$\bar{\mathbf{x}}_q = [\bar{x}_{qM}, \bar{x}_{qM+1}, \dots, \bar{x}_{qM+M-1}]^T.$$

Rewrite the vectors $\{\bar{\mathbf{x}}_q\}_{q=0}^{L-1}$, as a size N row vector, which is

$$[\bar{x}_0, \bar{x}_1, \dots, \bar{x}_{N-1}] = [\bar{\mathbf{x}}_0^T, \bar{\mathbf{x}}_1^T, \dots, \bar{\mathbf{x}}_{L-1}^T].$$

As in conventional OFDM, CP is added to this size- N row vector. Assuming that the length of CP is P , to avoid the inter-block-interference, P should satisfy $P > D$, where D is the maximum delay of the multipath channel. Without loss of generality, we assume that P is a multiple of the VB size M , i.e., $P = KM$. Then, after adding CP, the transmitted symbol sequence in the time domain can be written as ¹

$$[\bar{\mathbf{x}}_{L-K}^T, \bar{\mathbf{x}}_{L-K+1}^T, \dots, \bar{\mathbf{x}}_{L-1}^T, \bar{\mathbf{x}}_0^T, \bar{\mathbf{x}}_1^T, \dots, \bar{\mathbf{x}}_{L-1}^T]. \quad (1)$$

At the receiver, after removing CP, the received signal is the circular convolution of the transmitted signal and the CIR (Channel Impulse Response), which can be written as

$$\bar{y}_n = \sum_{d=0}^D h_d \bar{x}_{(n-d)_N} + w_n, \quad n = 0, 1, \dots, N-1,$$

where $\{h_d\}_{d=0}^D$ is the CIR, $w_n \sim \mathcal{CN}(0, \sigma^2)$ is the AWGN, and $(n)_N$ means $n \bmod N$. The receiver then divides the length N block $[\bar{y}_0, \bar{y}_1, \dots, \bar{y}_{N-1}]$ into L size M column vectors $\{\bar{\mathbf{y}}_q\}_{q=0}^{L-1}$, where $\bar{\mathbf{y}}_q$ is

$$\bar{\mathbf{y}}_q = [\bar{y}_{qM}, \bar{y}_{qM+1}, \dots, \bar{y}_{qM+M-1}]^T.$$

¹For large M , the CP length P may be smaller than M . In this case, we just move part of the symbols in the last VB to the front as the CP, and the notation of the transmitted symbol may be different from the equation (1).

Taking component-wise vector FFT of size L , we have

$$\mathbf{y}_l = \sum_{q=0}^{L-1} \bar{\mathbf{y}}_q e^{-j\frac{2\pi ql}{L}}, \quad l = 0, 1, \dots, L-1.$$

Write the length M column vector \mathbf{y}_l as

$$\mathbf{y}_l = [y_{lM}, y_{lM+1}, \dots, y_{lM+M-1}]^T.$$

We call \mathbf{y}_l the l -th receive VB.

Denote

$$H_k = \sum_{d=0}^D h_d e^{-j\frac{2\pi kd}{N}}, \quad k = 0, 1, \dots, N-1, \quad (2)$$

i.e., the frequency domain channel coefficient at the k -th subcarrier in conventional OFDM with size N FFT/IFFT. Define the $M \times M$ diagonal matrix $\bar{\mathbf{H}}_l$ as

$$\bar{\mathbf{H}}_l = \text{diag}\{H_l, H_{l+L}, \dots, H_{l+(M-1)L}\}. \quad (3)$$

Assuming perfect synchronization, with some signal processing manipulations [12] [13], the transmit VB \mathbf{x}_l and the receive VB \mathbf{y}_l have the relation

$$\mathbf{y}_l = \mathbf{H}_l \mathbf{x}_l + \mathbf{w}_l, \quad l = 0, 1, \dots, L-1, \quad (4)$$

where $\mathbf{w}_l = [w_{l,0}, w_{l,1}, \dots, w_{l,M-1}]^T$ is the noise vector, whose entries are i.i.d. and $\mathcal{CN}(0, \sigma^2)$ distributed, and the equivalent channel matrix \mathbf{H}_l can be expressed as

$$\mathbf{H}_l \triangleq \mathbf{U}_l^H \bar{\mathbf{H}}_l \mathbf{U}_l,$$

where \mathbf{U}_l is a unitary matrix, whose entry in the s -th row ($s = 0, 1, \dots, M-1$) and m -th ($m = 0, 1, \dots, M-1$) column equals

$$[\mathbf{U}_l]_{s,m} = \frac{1}{\sqrt{M}} \exp\left(-j\frac{2\pi(l+sL)m}{N}\right).$$

It is not difficult to verify that \mathbf{U}_l can be written as a product of a DFT matrix and a diagonal matrix, i.e.,

$$\mathbf{U}_l = \mathbf{F}_M \mathbf{\Lambda}_l,$$

where \mathbf{F}_M is the $M \times M$ DFT matrix and $\mathbf{\Lambda}_l$ is defined as

$$\mathbf{\Lambda}_l \triangleq \text{diag}\left\{1, e^{-j2\pi l/N}, e^{-j2\pi 2l/N}, \dots, e^{-j2\pi(M-1)l/N}\right\}. \quad (5)$$

Assuming that $\mathbb{E}\{|x_n|^2\} = 1$, $n = 0, 1, \dots, N-1$, the transmit SNR can be defined as $\rho \triangleq 1/\sigma^2$.

Note that although the CP overhead of the V-OFDM above is not changed, the IFFT size is reduced from N to L by M times. This IFFT size reduction also reduces the PAPR. In V-OFDM, if we choose parameter $M = 1$, then the received signal model (4) is exactly equivalent to the conventional OFDM. If we choose parameter $M = N$, then the signal model (4) is exactly equivalent to SC-FDE. When $L \neq N$ and $M \neq N$, V-OFDM can be treated as an implementation of signal space diversity (or modulation diversity) [14] [19].

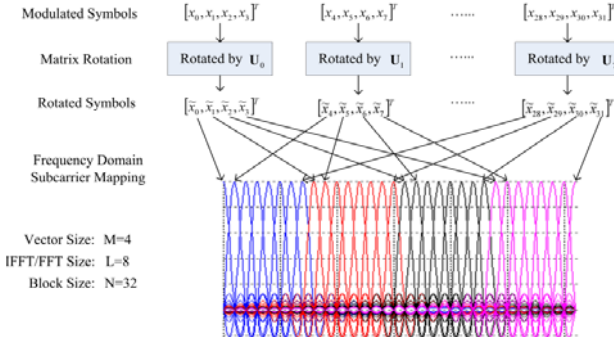


Fig. 1. V-OFDM modulation and mapping

III. DETECTION ALGORITHMS

In this section, we derive different detection algorithms for V-OFDM, assuming that the channel is perfectly known by the receiver.

A. ML Detection

Based on (4), the ML detection can be written as

$$\hat{\mathbf{x}}_l^{ML} = \arg \min_{\mathbf{x}_l} \|\mathbf{y}_l - \mathbf{H}_l \mathbf{x}_l\|^2, \quad l = 0, 1, \dots, L-1.$$

Clearly, complexity of ML-V-OFDM grows exponentially with the VB size M and the modulation order. In [16], the authors observed that different VBs may have different performances and further proposed a constellation rotation scheme to ensure consistent performance over different VBs. In [12] [17], the authors analyzed the performance of ML-V-OFDM, and in [17], it is shown that the majority of the VBs can achieve the maximum diversity order, which equals $\min\{M, D+1\}$.

B. ZF Detection

The equivalent channel matrix \mathbf{H}_l in (4) is the multiplication of two unitary matrices and a diagonal matrix, so its inversion is simple to calculate, which is

$$\begin{aligned} \mathbf{C}_l^{ZF} &\triangleq \mathbf{H}_l^{-1} = \mathbf{U}_l^H \bar{\mathbf{H}}_l^{-1} \mathbf{U}_l \\ &= \mathbf{U}_l^H \text{diag} \left\{ \frac{1}{H_l}, \frac{1}{H_{l+L}}, \dots, \frac{1}{H_{l+(M-1)L}} \right\} \mathbf{U}_l. \end{aligned}$$

The signal after the ZF processing is

$$\begin{aligned} \hat{\mathbf{y}}_l^{ZF} &= \mathbf{C}_l^{ZF} \mathbf{y}_l = \mathbf{x}_l + \mathbf{C}_l^{ZF} \mathbf{w}_l \\ &\triangleq [\hat{y}_{lM}^{ZF}, \hat{y}_{lM+1}^{ZF}, \dots, \hat{y}_{lM+M-1}^{ZF}]^T, \end{aligned} \quad (6)$$

and the symbol-by-symbol detection is

$$\hat{x}_n^{ZF} = \arg \min_{x_n} |\hat{y}_n^{ZF} - x_n|^2, \quad n = 0, 1, \dots, N-1. \quad (7)$$

The noise covariance of the signal after ZF processing can be calculated as

$$\begin{aligned} \mathbf{R}_w^{ZF} &= \mathbb{E} [\mathbf{C}_l^{ZF} \mathbf{w}_l \mathbf{w}_l^H (\mathbf{C}_l^{ZF})^H] \\ &= \mathbf{U}_l^H \text{diag} \left\{ \frac{\sigma^2}{|H_l|^2}, \frac{\sigma^2}{|H_{l+L}|^2}, \dots, \frac{\sigma^2}{|H_{l+(M-1)L}|^2} \right\} \mathbf{U}_l. \end{aligned}$$

Because $\mathbf{U}_l = \mathbf{F}_M \mathbf{\Lambda}_l$, where \mathbf{F}_M is a DFT matrix and $\mathbf{\Lambda}_l$ is a diagonal matrix defined in (5), it is not difficult to see that the diagonal elements in \mathbf{R}_w^{ZF} are equal, and can be written as

$$[\mathbf{R}_w^{ZF}]_{m,m} = \frac{1}{M} \sum_{n=0}^{M-1} \frac{\sigma^2}{|H_{l+nL}|^2}, \quad m = 0, 1, \dots, M-1.$$

Since the ZF estimation is unbiased, and $\mathbb{E}[x_n] = 1$, for $n = 0, 1, \dots, N-1$, we have that the detection SNR for the m -th element in the l -th VB \mathbf{x}_l is

$$\rho_{l,m}^{ZF} \triangleq \frac{\mathbb{E}[x_{lM+m}]}{[\mathbf{R}_w^{ZF}]_{m,m}} = \left[\frac{1}{M} \sum_{k=0}^{M-1} \frac{1}{\rho |H_{l+kL}|^2} \right]^{-1}, \quad (8)$$

and $\rho_{l,0}^{ZF} = \rho_{l,1}^{ZF} = \dots = \rho_{l,M-1}^{ZF} \triangleq \rho_l^{ZF}$.

ZF-V-OFDM has a simple matrix inversion and simple symbol-by-symbol detection. Its complexity does not increase with the VB size M , and is much lower than that of ML-V-OFDM.

IV. THE PERFORMANCE INDEPENDENCE OF VECTOR BLOCK INDEX l

Since ZF-V-OFDM use scalar detectors as in (7), their performances depend only on the distributions of the detection SNRs, i.e., ρ_l^{ZF} . According to (8), we can see that the distributions of the detection SNRs further depend on the joint PDF of the channel coefficients $\{H_{l+mL}\}_{m=0}^{M-1}$.

Define $\mathbf{h} \triangleq [h_0, h_1, \dots, h_D]^T$ and $\bar{\mathbf{h}}_l \triangleq [H_l, H_{l+L}, \dots, H_{l+(M-1)L}]^T$. Based on (2), $\bar{\mathbf{h}}_l$ can be written as

$$\bar{\mathbf{h}}_l = \mathbf{Q}_l \mathbf{h}, \quad l = 0, 1, \dots, L-1,$$

where \mathbf{Q}_l is an $M \times (D+1)$ matrix, whose element in the m -th row and d -th column equals $[\mathbf{Q}_l]_{m,d} = \frac{1}{\sqrt{M}} \exp(-j2\pi(l+mL)d/N)$, where $m = 0, 1, \dots, M-1$ and $d = 0, 1, \dots, D$.

The following lemma shows that the joint PDF of the elements in $\bar{\mathbf{h}}_l$ is independent of l .

Lemma 1: Assume that the elements in \mathbf{h} are independent and zero mean complex Gaussian distributed, $\bar{\mathbf{h}}_l = \mathbf{Q}_l \mathbf{h}$ and \mathbf{Q}_l is defined as $[\mathbf{Q}_l]_{m,d} = \frac{1}{\sqrt{M}} \exp(-j2\pi(l+mL)d/N)$, where $l = 0, 1, \dots, L-1$, $m = 0, 1, \dots, M-1$ and $d = 0, 1, \dots, D$. Then, the joint PDF of the elements in $\bar{\mathbf{h}}_l$ is independent of l .

Proof: Since $\bar{\mathbf{h}}_l$ is a linear combination of \mathbf{h} and the elements in \mathbf{h} are Gaussian distributed, the elements in $\bar{\mathbf{h}}_l$ are also Gaussian distributed and the PDF is fully determined by the mean and covariance of $\bar{\mathbf{h}}_l$. Because \mathbf{h} is zero mean, so is $\bar{\mathbf{h}}_l$. The covariance of $\bar{\mathbf{h}}_l$ can be calculated as

$$\mathbf{R}_{\bar{\mathbf{h}}_l} \triangleq \mathbb{E}_{\mathbf{h}} [\bar{\mathbf{h}}_l \bar{\mathbf{h}}_l^H] = \mathbf{Q}_l \mathbb{E}_{\mathbf{h}} [\mathbf{h} \mathbf{h}^H] \mathbf{Q}_l^H = \mathbf{Q}_l \mathbf{R}_{\mathbf{h}} \mathbf{Q}_l^H,$$

where $\mathbf{R}_{\mathbf{h}} \triangleq \mathbb{E}_{\mathbf{h}} [\text{diag}\{|h_0|^2, |h_1|^2, \dots, |h_D|^2\}]$. The matrix \mathbf{Q}_l can be written as

$$\mathbf{Q}_l = \mathbf{Q}_0 \tilde{\mathbf{\Lambda}}_l,$$

where $\tilde{\Lambda}_l \triangleq \text{diag}\{1, e^{-j2\pi l/N}, \dots, e^{-j2\pi D l/N}\}$. So, we have

$$\mathbf{R}_{\tilde{\mathbf{h}}_l} = \mathbf{Q}_0 \tilde{\Lambda}_l \mathbf{R}_{\mathbf{h}} \tilde{\Lambda}_l^H \mathbf{Q}_0^H.$$

It is not difficult to see that $\tilde{\Lambda}_l \mathbf{R}_{\mathbf{h}} \tilde{\Lambda}_l^H = \mathbf{R}_{\mathbf{h}}$ and

$$\mathbf{R}_{\tilde{\mathbf{h}}_l} = \mathbf{Q}_0 \mathbf{R}_{\mathbf{h}} \mathbf{Q}_0^H,$$

which means that $\mathbf{R}_{\tilde{\mathbf{h}}_l}$ is independent of l . Since it is Gaussian distributed, we have that the PDF of the elements in $\tilde{\mathbf{h}}_l$ does not depend on l . ■

According to (8) and Lemma 1, we have the following theorem.

Theorem 1: For ZF-V-OFDM, after averaging over the channel, all the N transmitted symbols $\{x_n\}_{n=0}^{N-1}$ have the same error rate performance.

So, in the following, we focus on the performance analysis of one VB only, without loss of generality, we assume it is $l = 0$, and the performance result is valid for all $l = 0, 1, \dots, L-1$.

V. DIVERSITY ANALYSIS V-OFDM WITH ZF RECEIVER

The SER can be calculated as the pair-wise error probability averaged over the channel and the transmitted symbols, which can be written as

$$P_{ser}(R, M, D, N) \triangleq \mathbb{E}_{\mathbf{H}_l, x_n, x_m} \{P(x_n \rightarrow x_m | \mathbf{H}_l, x_n \neq x_m)\}.$$

The SER depends on parameters R (the transmission rate in bits/symbol, or spectrum efficiency), M (the size of VB), D (the channel length), and N (the V-OFDM symbol length). The diversity order is defined as

$$d(R, M, D, N) = - \lim_{\rho \rightarrow \infty} \frac{\log P_{ser}(R, M, D, N)}{\log \rho}.$$

We use $d^{ZF}(R, M, D, N)$ to represent the diversity orders of ZF-V-OFDM.

Following the same approach as in [18] [?], we can define the effective mutual information between the linear filter output \hat{y}_l and the transmitted symbol \mathbf{x}_l as

$$I(\hat{y}_l; \mathbf{x}_l) = \frac{1}{M} \sum_{m=0}^{M-1} I(\hat{y}_{lM+m}; x_{lM+m}). \quad (9)$$

Due to (8), for ZF-V-OFDM, $I(\hat{y}_{lM+m}, x_{lM+m})$ can be written as

$$\begin{aligned} I^{ZF}(\hat{y}_{lM+m}; x_{lM+m}) &= \log(1 + \rho_l^{ZF}) \\ &= \log \left(1 + \left(\frac{1}{M} \sum_{n=0}^{M-1} \frac{1}{\rho |H_{l+nL}|^2} \right)^{-1} \right). \end{aligned} \quad (10)$$

Because the detection SNRs of all the symbols in one VB are the same, the mutual information in (9) equals to the mutual information of each symbol in one VB, i.e.,

$$\begin{aligned} I^{ZF}(\hat{y}_l; \mathbf{x}_l) &= I^{ZF}(\hat{y}_{lM+m}; x_{lM+m}) \\ &= \log \left(1 + \left(\frac{1}{M} \sum_{n=0}^{M-1} \frac{1}{\rho |H_{l+nL}|^2} \right)^{-1} \right). \end{aligned} \quad (11)$$

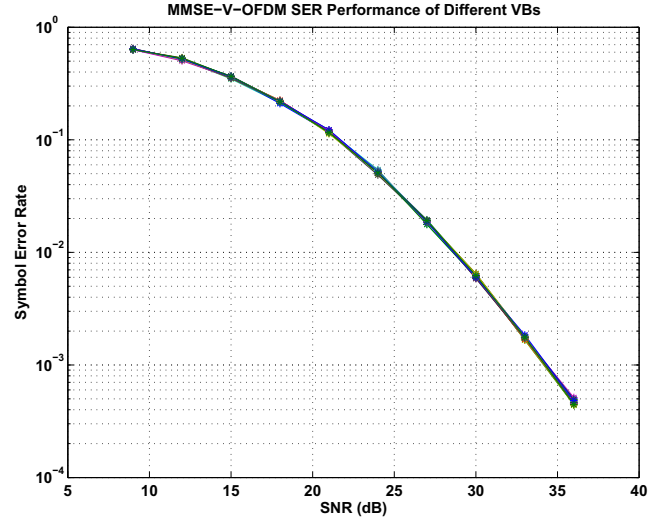


Fig. 2. MMSE-V-OFDM SER performance of different VBs at $M = 64$, $D = 2$ and 16QAM.

The outage probability is defined as

$$P_{out}(R, M, D, N) \triangleq P[I(\hat{y}_l, \mathbf{x}_l) < R], \quad (12)$$

which is equal to $P[I(\hat{y}_{lM+m}; x_{lM+m}) < R]$ for ZF-V-OFDM. This means that the above outage probability of the detection of the vector channel (4) after the ZF operator/receiver is indeed that of the scalar channel detection (7). Similarly, the outage diversity order is defined as

$$d_{out}(R, M, D, N) = - \lim_{\rho \rightarrow \infty} \frac{\log P_{out}(R, M, D, N)}{\log \rho}.$$

Also, we use $d_{out}^{ZF}(R, M, D, N)$ to represent the outage diversity order for ZF-V-OFDM.

Similarly as in [18] [?], we define the exponential equal of two functions $f(\rho)$ and $g(\rho)$, write it as $f(\rho) \doteq g(\rho)$, if

$$\lim_{\rho \rightarrow \infty} \frac{\log f(\rho)}{\log \rho} = \lim_{\rho \rightarrow \infty} \frac{\log g(\rho)}{\log \rho}.$$

If ZF receiver is used for V-OFDM, the diversity order only equals 1. This is summarized in the following theorem.

Theorem 2: For ZF-V-OFDM, the diversity order $d^{ZF}(R, M, D, N) = 1$.

Proof: Substituting (10) into $P_{out}(R, M, D, N)$ (12) and following the same procedure as that used in [18] to prove the Theorem 4, we can show that $d_{out}^{ZF}(R, M, D, N) = 1$. Similarly, we can show that $d^{ZF}(R, M, D, N) = 1$. ■

VI. SIMULATION RESULTS

In this section, we do simulations to validate the analysis. In all the simulations, we assume that the V-OFDM symbol length $N = 1024$, the CP length $P = 128$, and the channel CIR is a length $D+1$ vector which has i.i.d. complex Gaussian distributed elements. For all the SER plots, the system is uncoded. $R = 2, 4$, and 6 represent QPSK, 16QAM, and 64QAM, respectively.

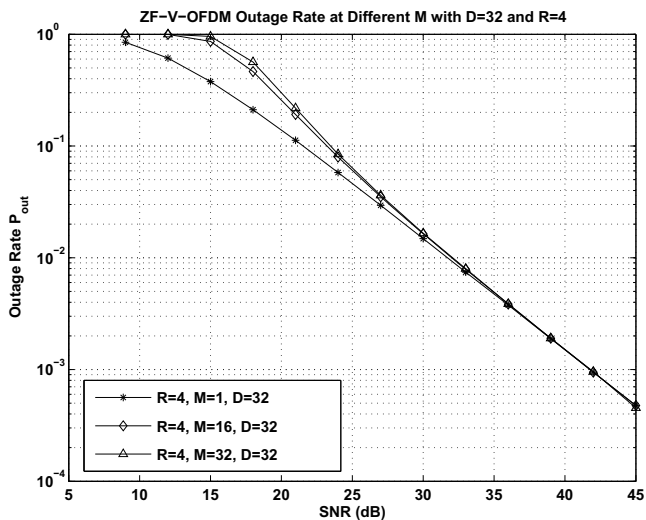


Fig. 3. ZF-V-OFDM outage rate at different M .

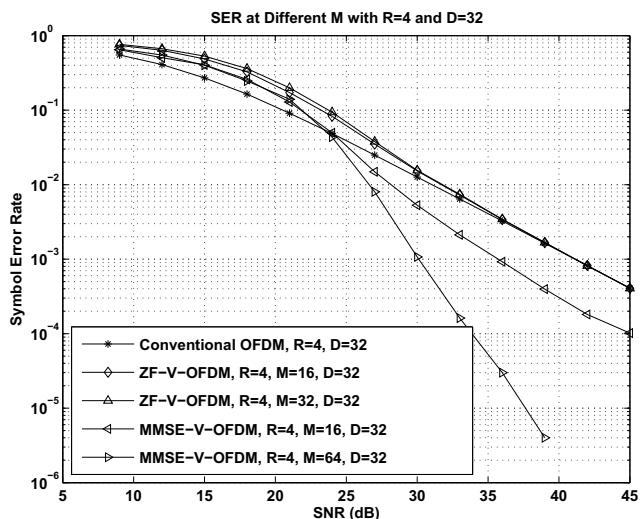


Fig. 4. SER comparison between conventional OFDM, MMSE-V-OFDM and ZF-V-OFDM.

To verify Theorem 1, Fig.2 plots the SER vs. SNR for different VBs when MMSE-V-OFDM is used. The parameters assumed in the plots are: $(R, M) = (4, 64)$, and $D = 2$. In this case, there are totally $L = N/M = 1024/64 = 16$ VBs. In the figure, we plot 16 curves. The equal performance can be clearly seen from the overlaps of the curves for different VBs. Also, it is worth noticing that for ML-V-OFDM, due to the complexity, it is difficult to run simulation for large M , while for MMSE-V-OFDM, we can get the simulation results for large M easily. For ZF-V-OFDM, we have similar results.

Fig.3 shows the outage rate of ZF-V-OFDM at different M with $D = 32$ and $R = 4$. We can see that ZF-V-OFDM does not provide any diversity gain.

Fig.4 compares the SER performance of conventional OFDM (i.e., V-OFDM with $M = 1$) MMSE-V-OFDM (i.e.,

V-OFDM with MMSE receiver) and ZF-V-OFDM at different M , with $D = 32$ and $R = 4$. From the plot, we can see that, when M is increasing, the ZF-V-OFDM does not have any diversity gain, and it is equivalent to the conventional OFDM at high SNR. In comparison, for MMSE-V-OFDM, when $M = 16$ and 64 , $\lfloor M2^{-R} \rfloor = 1$ and 4 , and the diversity order equals 2 and 5, respectively. From the plot, we can clearly see the better performance of MMSE-V-OFDM.

VII. CONCLUSIONS

In this paper, we analyzed the performance of V-OFDM with ZF receivers. We showed that for the ZF-V-OFDM, all the VBs have the same performance. This is different from ML-V-OFDM. Also, different from ML-V-OFDM, the complexity of ZF-V-OFDM does not increase with the size of VB. We showed that ZF-V-OFDM does not provide any diversity gain.

VIII. ACKNOWLEDGEMENT

The work of Yabo Li and Ibo Ngeban is supported by the National Science Foundation of China (NSFC) under Grant 61010197, Chinese Ministry of Education New Faculty Fund under Grant 20100101120039, National Science and Technology Major Project under Grant 2011ZX03003-003-03, and National Key Basic Research Program of China under grant 2012CB316104.

The work of X.-G. Xia is supported in part by the National Science Foundation (NSF) under Grant CCF-0964500 and the World Class University (WCU) Program, National Research Foundation, Korea.

REFERENCES

- [1] L. J. Cimini, "Analysis and simulation of a digital mobile channel using orthogonal frequency division multiplexing," *IEEE Trans. on Commun.*, vol. COM-33, no. 7, pp. 665-675, July 1985.
- [2] J. A. C. Bingham, "Multicarrier modulation for data transmission: an idea whose time has come," *IEEE Commun. Mag.*, vol. 28, no. 5, pp. 5-14, May 1990.
- [3] 802.16m/D5, Draft Amendment to IEEE Standard for Local and Metropolitan Area Networks Part 16: Air Interface for Fixed and Mobile Broadband Wireless Access Systems.
- [4] 3GPP TS 36.211, Evolved Universal Terrestrial Radio Access (E-UTRA), Physical Channels and Modulation, Release 10, v10.1.0 (2011-03).
- [5] "IEEE 802.11ad standard draft D0.1," [Available] http://www.ieee802.org/11/Reports/tgad_update.htm.
- [6] S. H. Han and J. H. Lee, "An overview of peak-to-average power ratio reduction techniques for multicarrier transmission," *IEEE Trans. on Wireless Commun.*, vol. 12, no. 2, pp. 56-65, Apr. 2005.
- [7] H. Sari, G. Karam, and I. Jeanclaude, "Transmission techniques for digital terrestrial TV broadcasting," *IEEE Commun. Mag.*, pp. 100-109, Feb. 1995.
- [8] M. V. Clark, "Adaptive frequency-domain equalization and diversity combining for broadband wireless communications," *IEEE J. Select. Areas Commun.*, vol. 16, pp. 1385-1395, Oct. 1998.
- [9] N. Al-Dhahir, "Single-carrier frequency-domain equalization in frequency-selective fading channels," *IEEE Commun. Lett.*, vol. 7, no. 7, pp.304-306, July 2001.
- [10] D. Falconer, S. L. Ariyavisitakul, A. Benyamin-Seeyar, and B. Eidson, "Frequency domain equalization for single-carrier broadband wireless systems," *IEEE Commun. Mag.*, vol. 40, no. 4, pp. 58-66, Apr. 2002.
- [11] C. Ciochina and H. Sari, "A review of OFDMA and single-carrier FDMA," in *Proc. of 2010 European Wireless Conference*, pp. 706-710, 12-15 Apr. 2010.
- [12] X.-G. Xia, "Precoded and vector OFDM robust to channel spectral nulls and with reduced cyclic prefix length in single transmit antenna systems," *IEEE Trans. on Commun.*, vol. 49, no. 8, pp. 1363-1374, Aug. 2001.

- [13] H. Zhang, X.-G. Xia, L. J. Cimini, and P. C. Ching, "Synchronization techniques and guard-band-configuration scheme for single-antenna vector-OFDM systems," *IEEE Trans. on Wireless Commun.*, vol. 4, no. 5, pp. 2454-2464, Sept. 2005.
- [14] H. Zhang and X.-G. Xia, "Iterative decoding and demodulation for single-antenna vector OFDM systems," *IEEE Trans. on Veh. Tech.*, vol. 55, no. 4, pp. 1447-1454, Jul. 2006.
- [15] H. Zhang, X.-G. Xia, Q. Zhang, and W. Zhu, "Precoded OFDM with adaptive vector channel allocation for scalable video transmission over frequency-selective fading channels," *IEEE Trans. on Mobile Comp.*, vol. 1, no. 2, pp. 132-141, Apr.-Jun. 2002.
- [16] C. Han, T. Hashimoto, and N. Suehiro, "Constellation-rotated vector OFDM and its performance analysis over Rayleigh fading channels," *IEEE Trans. on Commun.*, vol. 58, no. 3, pp. 828-837, Mar. 2010.
- [17] P. Cheng, M. Tao, Y. Xiao, and W. Zhang, "V-OFDM: On performance limits over multi-path Rayleigh fading channels," *IEEE Trans. on Commun.*, vol. 59, no. 7, pp. 1878-1892, Jul. 2011.
- [18] A. Tajer and A. Nosratinia, "Diversity order in ISI channels with single-carrier frequency-domain equalizers," *IEEE Trans. on Wireless Commun.*, vol. 9, no. 3, pp. 1022-1032, Mar. 2010.
- [19] J. Boutros and E. Viterbo, "Signal space diversity: a power- and bandwidth-efficient diversity technique for the Rayleigh fading channel," *IEEE Trans. on Inf. Theory*, vol. 44, no. 4, pp. 1453-1467, Jul. 1998.